Electronic Supplementary Information

Facile syntheses, structures and photocatalytic properties of 3-D iodoargentate frameworks derived from TM-flexible-amino-ligand templates

Yan Gao, Xiao Yang, Taohong Ren, Dingxian Jia*

College of Chemistry, Chemical Engineering and Materials Science, Soochow University, Suzhou 215123, People's Republic of China.

Table of Contents

Table S1 Crystallographic and refinement data of **1**-**3**

	1	**2**	**3**
Empirical formula	$C_6H_{24}N_6CoAg_2I_4$	$C_6H_{24}N_6FeAg_2I_4$	$C_8H_{28}N_6OCoAg_2I_4$
Fw	962.58	959.50	1006.63
Crystal system	hexagonal	hexagonal	tetragonal
Space group	$P6_322$	$P6_322$	$I4_1/amd$
a / Å	9.0389(11)	9.0851(11)	21.681(4)
b / Å	9.0389(11)	9.0851(11)	21.681(4)
c / Å	14.437(3)	14.411(3)	9.2216(19)
α / °	90	90	90
β / °	90	90	90
γ / °	120	120	90
V / Å^3	1021.5(3)	1030.1(3)	4334.6(19)
Z	2	2	4
T / K	293(2)	293(2)	293(2)
D_c/Mg·m^{-3}	3.130	3.093	1.543
F(000)	870	868	1836
2θ(max) / °	50.70	50.70	50.70
Measured reflections	9919	2488	19638
Unique reflections	634	633	1056
R_{int}	0.0413	0.0308	0.0949
No.of parameters	33	37	35
R_1 [I>2σ(I)]	0.0240	0.0235	0.0430
wR_2 (all data)	0.0551	0.0501	0.1053
Goodness of fit	1.273	1.122	1.085

Table S2. Selected Bond Lengths (Å) and angles (°) for **1**

Ag(1)–I(1)	2.8574(5)	Ag(1)–I(2)	2.8818(13)
Co(1)–N(1)	2.169(6)		
I(1)–Ag(1)–I(1)#2	113.752(19)	I(1)–Ag(1)–I(2)	104.75(2)
Ag(1)–I(1)#3–Ag(1)	142.89(3)	Ag(1)–I(2)–Ag(1)	180.0
N(1)#6–Co(1)–N(1)	92.7(4)	N(1)#5–Co(1)–N(1)#4	93.7(2)
N(1)#5–Co(1)–N(1)#6	171.6(4)	N(1)#1–Co(1)–N(1)#6	80.5(4)

Symmetry transformations used to generate equivalent atoms: #1) –y+1, –x+1, –z+1/2; #2) –y+1, x–y+1, z; #3) –x+y, –x+1, z; #4) –y+1, x–y–1, z; #5) x, x–y–1, –z+1/2; #6) –x+y+2, y, –z+1/2.

Table S3. Selected Bond Lengths (Å) and angles (°) for **2**

Ag(1)–I(1)	2.8592(5)	Ag(1)–I(2)	2.8758(12)
Fe(1)–N(1)	2.214(6)		
I(1)#1–Ag(1)–I(1)	113.767(16)	I(1)–Ag(1)–I(2)	104.73(2)
Ag(1)–I(2)–Ag(1)#2	180.0	Ag(1)#3–I(1)–Ag(1)	144.30(2)
N(1)–Fe(1)–N(1)#4	94.0(2)	N(1)–Fe(1)–N(1)#5	93.5(3)
N(1)–Fe(1)–N(1)#6	170.2(4)	N(1)#4–Fe(1)–N(1)#6	79.3(3)

Symmetry transformations used to generate equivalent atoms: #1) –y+1, x–y, z; #2) –y+1, –x+1, z–1/2; #3) x–y, –y+1, –z+2; #4) –y+1, x–y–1, z; #5) –x+y+2, y, –z+1/2; #6) x, x–y–1, –z+1/2.

Table S4. Selected Bond Lengths (Å) and angles (°) for **3**

Ag(1)–I(1)	2.899(3)	Ag(1)–I(2)#1	2.841(4)
Co(1)–N(1)	2.06(3)	Co(1)–N(2)#4	2.00(6)
I(1)–Ag(1)–I(1)	101.06(16)	I(2)#3–Ag(1)–I(1)#1	113.15(7)
I(2)#1–Ag(1)–I(2)#1	108.53(16)	I(2)#3–Ag(1)–I(1)#3	110.45(8)
Ag(1)–I(1)–Ag(1)#2	177.89(16)	Ag(1)#1–I(2)–Ag(1)	71.47(16)
N(1)#6–Co(1)–N(1)#4	91.0(3)	N(2)–Co(1)–N(1)#6	82.4(12)
N(1)#5–Co(1)–N(1)#4	165(2)	N(2)–Co(1)–N(1)#5	97.6(12)

Symmetry transformations used to generate equivalent atoms: #1) –x+1, –y+1, –z+1; #3) –y+1, x–y+1, z; #4) –y+3/4, x+1/4, z–1/4; #5) –y+1, –x+1, –z+1/2; #6) x–y, –y+1, –z; #7) –y+5/4, x+1/4, –z+3/4.

Table S5. Selected H···A distances(Å) and D–H···A angles (°) for **1-3**

D–H···A	d(H···A)	d(D···A)	<(DHA)
1			
N(1)–H(1B)···I(1)#1	3.041	3.842	150.71
C(1)–H(1D)···I(1)#2	3.154	3.895	134.33
2			
N(1)–H(1B)···I(1)#1	3.040	3.842	150.93
C(1)–H(1D)···I(1)#2	3.184	3.927	134.72
3			
N(1)–H(1A)···I(1)#1	2.993	3.803	152.17
N(1)–H(1B)···I(1)#2	2.993	3.803	152.17

Symmetry transformations used to generate equivalent atoms: For **1**: #1) -y+1, x-y, z; #2) x+1, y, z. For **2**: #1) -y+1, x-y, z-1; #2) x-y+1, x, z-1/2. For **1**: #1) -x+1, -y+1, -z+1; #2) y+1/4, -x+5/4, z-1/4.

Table S6. Summary of Catalytic Activities in Photodegradation of Organic Dyes for Some Iodoargentate Hybrids with Different Cations

Compound	organic dyes	light source	irradiation time	band gaps of hybrids	degradation ratio	Ref.
$(Et_2mbt)[Ag_2I_3]$	[d]MO	UV light	60 min	2.95 eV	94%	1
[a]$\{(Hmbt)[AgI]\}_n$	MO	UV light	80 min	2.78 eV	85%	
[b]$[(Hpy)(Ag_2I_3)]_n$	[e]RhB	Hg lamp	180 min	2.93 eV	89%	2
$\{[(Hpy)_2\cdot dmf][Ag_6I_8]\}_n$	RhB	Hg lamp	180 min	3.05 eV	93%	
$\{[(Hpy)_2\cdot H_2O][Ag_3I_5]\}_n$	RhB	Hg lamp	180 min	2.99 eV	83%	
$[(Hpy)(Ag_5I_6)]_n$	RhB	Hg lamp	180 min	2.71 eV	98%	
$Fe(2,2'\text{-bipy})_3]Ag_3I_5$	[f]CV	Xe lamp	60 min	1.87 eV	93%	3
$Ni(2,2'\text{-bipy})_3]Ag_3I_5$	CV	Xe lamp	60 min	2.01 eV	89%	
$Zn(2,2'\text{-bipy})_3]Ag_3I_5$	CV	Xe lamp	60 min	2.61 eV	56%	
$Mn(2,2'\text{-bipy})_3]Ag_3I_5$	CV	Xe lamp	60 min	2.28 eV	100%	
$[(Me)_2\text{-}2,2'\text{-bipy}]_2Ag_7I_{11}$	CV	Xe lamp	50 min	2.03 eV	100%	4
	RhB	Xe lamp	60 min	2.03 eV	100%	
$[Zn(2, 2'\text{-bipy})_3]Ag_5I_7$	CV	UV light	60 min	2.58 eV	98%	5
$[Ni(2, 2'\text{-bipy})_3]Ag_5I_7$	CV	UV light	60 min	2.10 eV	98%	
$[Co(2, 2'\text{-bipy})_3]Ag_5I_7$	CV	UV light	60 min	1.94 eV	98%	
[c]$K_x[TM(2,2'\text{-bipy})_3]_2Ag_6I_{11}$ (TM = Mn, Fe, Co, Ni, Zn)	CV	Xe lamp	50-60min	1.66 -2.08 eV	56-100%	6
$[(Ni(2,2'\text{-bipy})_3][H\text{-}2,2\text{-bipy}]Ag_3I_6$	CV	Xe lamp	60 min	2.75 eV	71%	
[c]$K_x[Mn(2,2'\text{-bipy})_3]_2Ag_6I_{11}$	RhB	Xe lamp	30min	2.01 eV	100%	
[c]$K_x[TM(2,2'\text{-bipy})_3]_2Ag_6I_{11}$ (TM = Fe, Co, Ni, Zn)	RhB	Xe lamp	180 min	1.66-2.08 eV	88-100%	
$[(Ni(2,2'\text{-bipy})_3][H\text{-}2,2\text{-bipy}]Ag_3I_6$	RhB	Xe lamp	180 min	2.75 eV	100%	
$[Co(phen)_3]Ag_3I_5\cdot 2CH_3CN$	RhB	Hg lamp	180 min	3.04 eV	51%	7
$[Co(phen)_3]_2Ag_{11}I_{15}\cdot H_2O$	RhB	Hg lamp	180 min	2.84 eV	62%	
$[Cu(phen)_3]_2Ag_{11}I_{15}\cdot H_2O$	RhB	Hg lamp	180 min	2.87 eV	80%	
$[Co(phen)_3]_2Ag_{13}I_{17}$	RhB	Hg lamp	180 min	2.89 eV	40%	
$[Cd(phen)_3]_2Ag_{13}I_{17}$	RhB	Hg lamp	180 min	3.19 eV	29%	
$[Ni(DMSO)_6][Ag_5I_7]$	[g]MV	UV light	150 min	2.73 eV	92%	8
$[V(DMSO)_5(H_2O)][Ag_6I_8]$	[h]MB	UV light	60 min	2.61 eV	100%	
[i]$[Fe(DMSO)_6][Ag_6I_9]\cdot DMSO$	MB	UV light	9 h	2.28 eV	90%	9
	MV	UV light	180 min	2.28 eV	80%	
$[Fe(H_2O)_6][Ag_{15}I_{18}]$	MB	UV light	240 min	1.92 eV	94%	
	MV	UV light	180 min	1.92 eV	90%	
[i]$[Cd(DMSO)_6][Ag_8I_{10}]$	MB	UV light	9 h	2.46 eV	91%	
	MV	UV light	180 min	2.46 eV	80%	
[j]$(EtPPh_3)Ag_3I_4$ (Et = ethyl)	RhB	Xe lamp	160 min	3.26 eV	80%	10
$(n\text{-}PrPPh_3)Ag_3I_4$ (n-Pr = n-propyl)	RhB	Xe lamp	160 min	3.37 eV	85%	
$(i\text{-}PrPPh_3)Ag_5I_6$ (i-Pr = isopropyl)	RhB	Xe lamp	160 min	2.76 eV	89%	
[k]$[Co(2,2'\text{-bipy})_3]Ag_3I_6$	CV	Xe lamp	120 min	2.03 eV	100%	11

	MB	Xe lamp	11 h	2.03 eV	100%	
	RhB	Xe lamp	120 min	2.03 eV	90%	
	MO	Xe lamp	8 h	2.03 eV	2%	
$[(Me)_2$-2,2′-bipy$]Ag_8I_{10}$ (Me = methyl)	RhB	Xe lamp	80 min	1.92 eV	95%	12
	MO	Xe lamp	60 min	1.92 eV	100%	
[l]$[La(DMA)_8]Ag_9I_{12}\cdot 2H_2O$	CV	Xe lamp	210 min	2.58 eV	27%	13
	RhB	Xe lamp	210 min	2.58 eV	68%	
$[Pr(DMA)_7]_2Ag_{16}I_{22}$	CV	Xe lamp	210 min	2.77 eV	80%	
	RhB	Xe lamp	210 min	2.77 eV	19%	
$[Sm(DMA)_7]_2Ag_{16}I_{22}$	CV	Xe lamp	210 min	2.74 eV	87%	
	RhB	Xe lamp	210 min	2.74 eV	37%	
[m]$[MBI][Ag_2I_3]$	RhB	Xe lamp	140 min	3.46 eV	60%	14
[n]$[MDMBI][Ag_2I_3]$	RhB	Xe lamp	140 min	3.31 eV	80%	
[o]$[Mn(2,2′\text{-bipy})_2(DMF)_2]Ag_5I_7$	CV	Xe lamp	6 h	2.68 eV	91%	15
$[\{Cd(2,2′\text{-bipy})_2\}_2(\mu_4\text{-}Ag_2I_6)]$	CV	Xe lamp	6 h	2.84 eV	28%	
[p]$[\{Zn(DMF)_2(H_2O)_2\}(4,4′\text{-bipy})_{1.5}]Ag_5I_7\cdot 2DMF$	CV	Xe lamp	6 h	2.75 eV	93%	
$[\{Nd(DMSO)_8\}(Ag_7I_{10})]_n$	MB	Xe lamp	80 min	3.04 eV	96%	16
$[\{Nd(DMSO)_8\}(Pb_2Ag_2I_9)]_n$	MB	Xe lamp	80 min	3.07 eV	90%	

[a]Hmbt = 2-mercaptobenzothiazole , [b]Hpy^+ = protonated pyridine, [c] x = 0.89−1, [d]MO methyl orange, [e]RhB = rhodamine B, [f]CV= crystal violet, [g]MV = methyl violet, [h]MB = methylene blue, [i] DMSO = dimethyl sulfoxide, [j]PPh_3 = aromatic triphenylphosphine, [k]2,2'- bipy = 2,2'-bipyridine, [l]DMA = N,N-dimethylacetamide, [m]MBI^+ = N,N-dimethylbenzimidazolium, [n]$MDMBI^+$ = N,N-dimethyl-5,6-dimethylbenzimidazolium, [o]DMF = N,N'-dimethylformamide, [p]4,4′-bipy = 4,4′-bipyridine.

[Reference]

1. G. N. Liu, K. Li, Q. S. Fan, H. Sun, X. Y. Li, X. N. Han, Y. Li, Z. W. Zhang, and C. Li, *Dalton Trans*. 2016, **45**, 19062–19071.
2. T. Yu, J. Shen, Y. Wang and Y. Fu, Eur. J. Inorg. Chem., 2015, 1989–1996.
3. X.-W. Lei, C.-Y. Yue, J.-Q. Zhao, Y.-F. Han, Z.-R. Ba, C. Wang, X.-Y. Liu, Y.-P. Gong and X.-Y. Liu, Eur. J. Inorg. Chem., 2015, 4412–4419.
4. X.-W. Lei, C.-Y. Yue, L.-J. Feng, Y.-F. Han, R.-R. Meng, J.-T. Yang, H. Ding, C.-S. Gao and C.-Y. Wang, CrystEngComm., 2016, **18**, 427–436.
5. X. W. Lei, C. Y. Yue, F. Wu, X. Y. Jiang, and L. N. Chen, *Inorg. Chem. Commun*. 2017, **77**, 64–67.
6. X. W. Lei, C. Y. Yue, J. Q. Zhao, Y. F. Han, J. T. Yang, R. R. Meng, C. S. Gao, H. Ding, C. Y. Wang, W. D. Chen, and M. C. Hong, *Inorg. Chem*. 2015, **54**, 10593−10603.
7. T. Yu, Y. Fu, Y. Wang, P. Hao, J. Shen and Y. Fu, CrystEngComm., 2015, **17**, 8752–8761.
8. Y. Mu, D. Wang, X. D. Meng, J. Pan, S. D. Han, and Z. Z. Xue, *Cryst. Growth Des*. 2020, **20,** 1130−1138.
9. Q. Wei, D. Wang, J. Pan, S. D. Han, and G. M. Wang. *Chem. Asian J*., 2019, **14**, 640−646.
10. G. N. Liu, X. Zhang, H. M. Wang, H. Xu, Z. H. Wang, X. L. Meng, Y. N. Dong, R. Y. Zhao, and C. C. Li. *Dalton Trans*., 2017, **46**, 12474−12486.
11. C. Y. Tang, Y. W. Sun, J. B. Liu, Q. F. Xu, C. Y. Zhang. *Dalton Trans*., 2022, **51**, 16784−16789.
12. C. Y. Yue, B. Hu, X. W. Lei, R. Q. Li, F. Q. Mi, H. Gao, Y. Li, F. Wu, C. L. Wang, and N. Lin. *Inorg. Chem*., 2017, **56**, 10962−10970.
13. Y. Gao, N. N. Chen, Y. M. Tian, J. H. Zhang, and D. X. Jia. *Inorg. Chem*., 2021, **60**, 3761−3772.
14. P. F. Hao, Y. Xu, X. Li, J. J. Shen, and Y. L. Fu. *Inorg. Chem. Front*., 2020, **7**, 3184−3194.
15. W. Zheng, Y. Gao, N. N. Chen, B. Wu, D. X. Jia, and S. X. Zhao. *Inorg. Chim. Acta*., 2020, **510**, 119762.
16. J. Y. Lu, J. H. Zhang, X. Yang, D. X. Jia, and S. X. Zhao. *Inorg. Chim. Acta*., 2022, **537**, 120962.

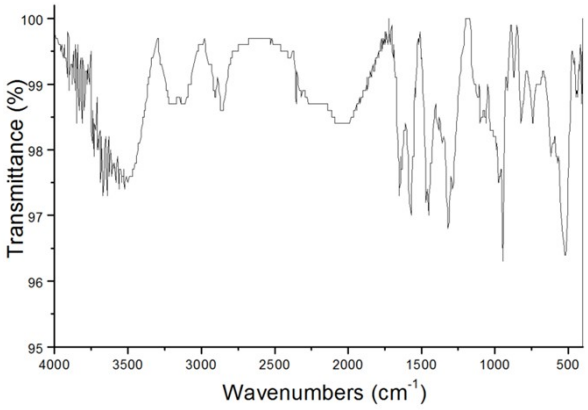

Fig. S1 IR spectrum of compound **1**.

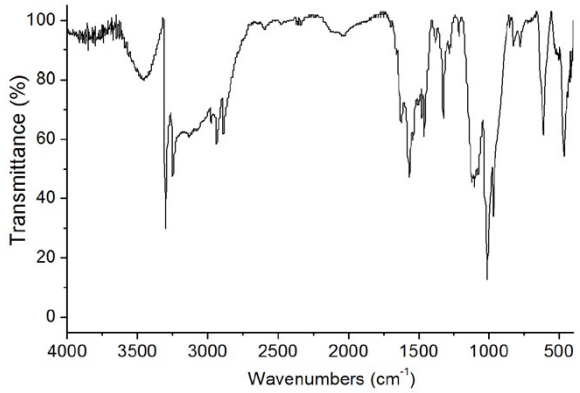

Fig. S2 IR spectrum of compound **2**.

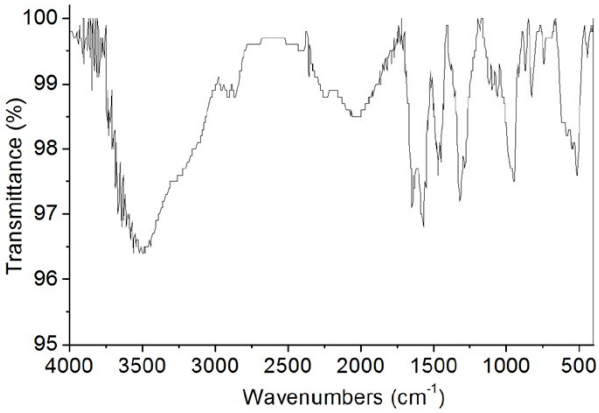

Fig. S3 IR spectrum of compound **3**.

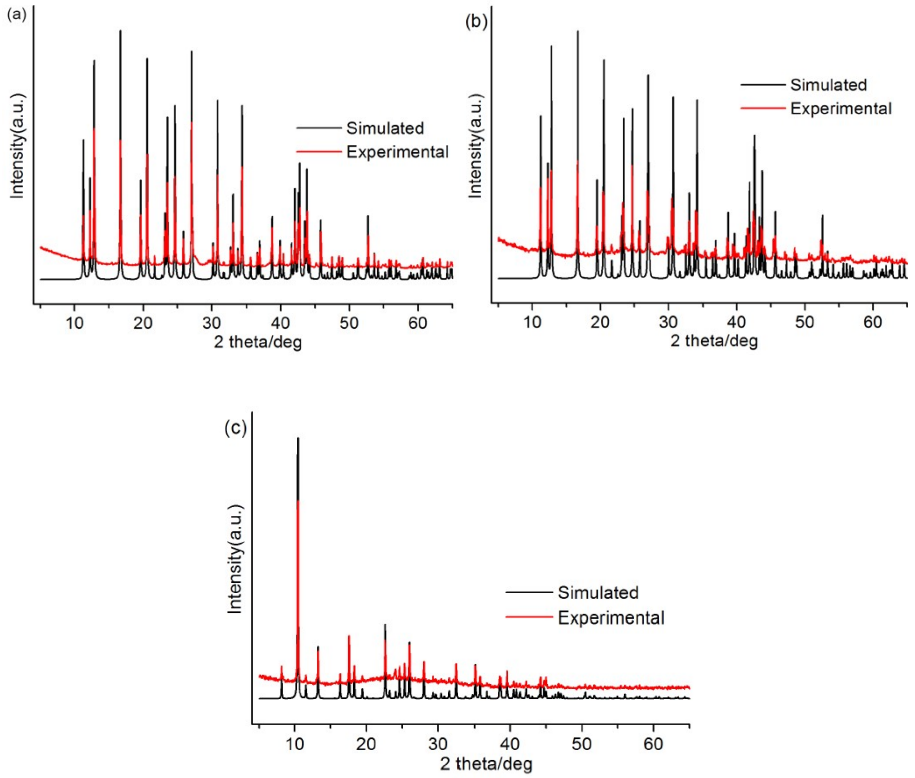

Fig. S4 Simulated and experimental powder XRD patterns of compound **1** (a), **2** (b) and **3** (c).

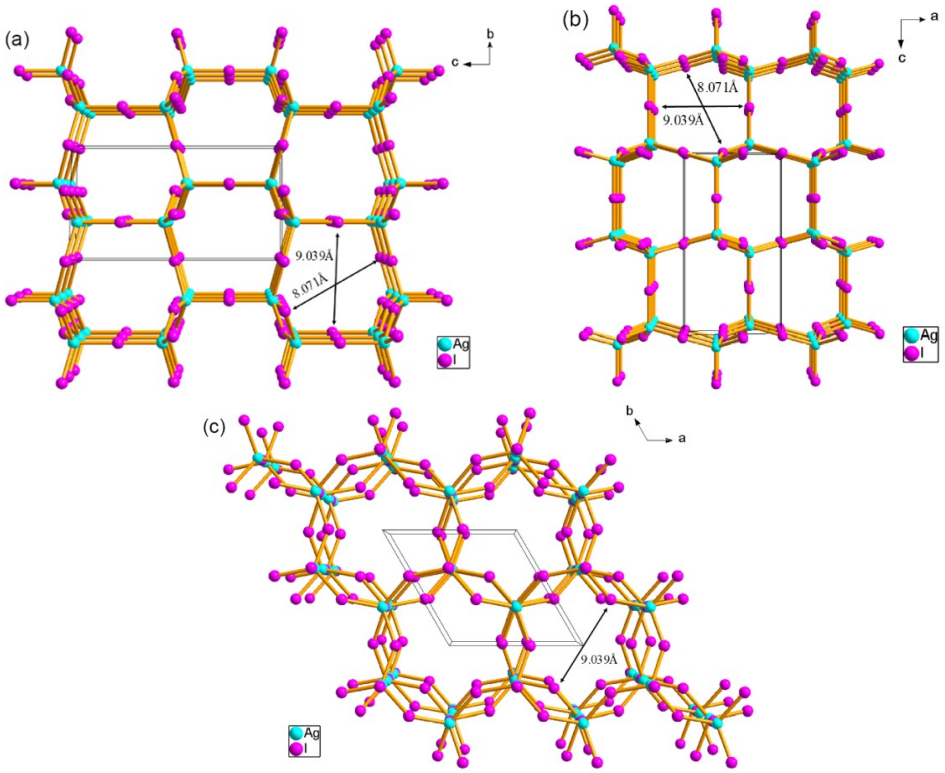

Fig. S5 Packing diagrams of **1** viewed along the *a* axis (a), *b* axis (b) and *c* axis (c) , showing cross-section size of the channels. $[Co(en)_3]^{2+}$ cations are omitted for clarity.

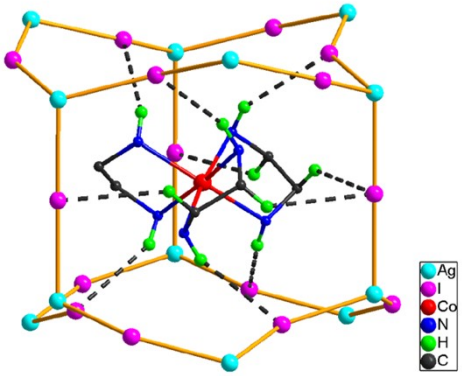

Fig. S6 A view of N–H···I and N–H···I H-bonding interaction between $[Co(en)_3]^{2+}$ and α-$[Ag_2I_4]_n^{2n-}$ framework in **1**.

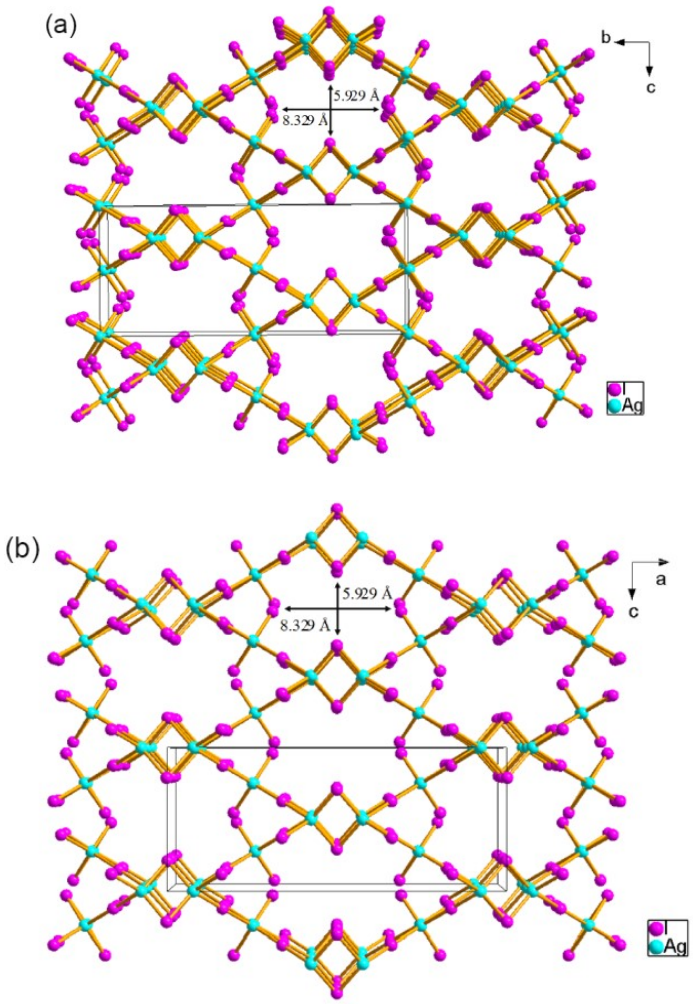

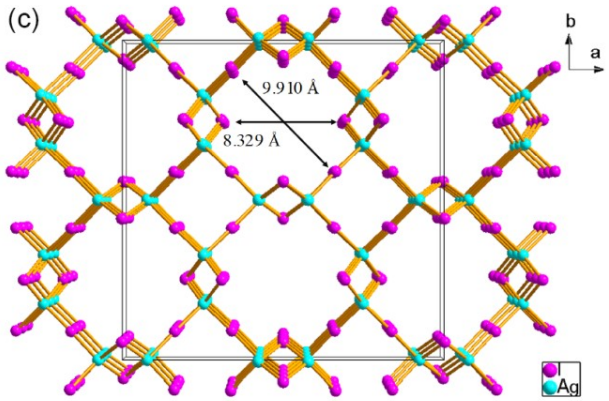

Fig. S7 Packing diagrams of **3** viewed along the *a* axis (a), *b* axis (b) and *c* axis (c), showing cross-section size of the channels. $[Co(dien)_2]^{2+}$ cations are omitted for clarity.

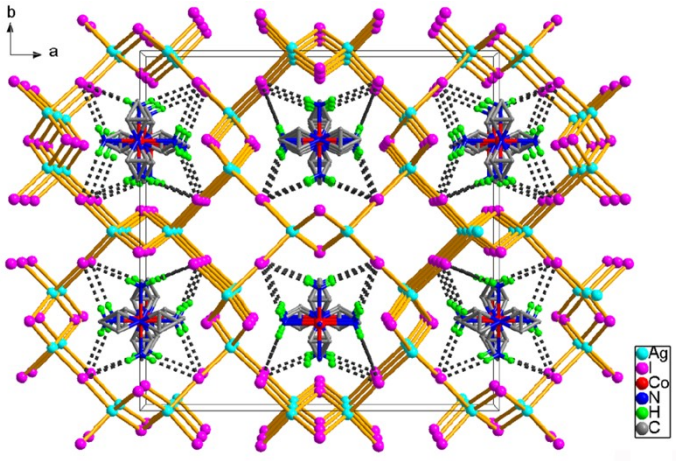

Fig. S8 A packing diagram of **3** viewed along the *c* axis, showing N–H···I H-bonding interactions between $[Co(dien)_2]^{2+}$ cation and β-$[Ag_2I_4]_n^{2n-}$ framework. H_2O molecules are omitted for clarity.

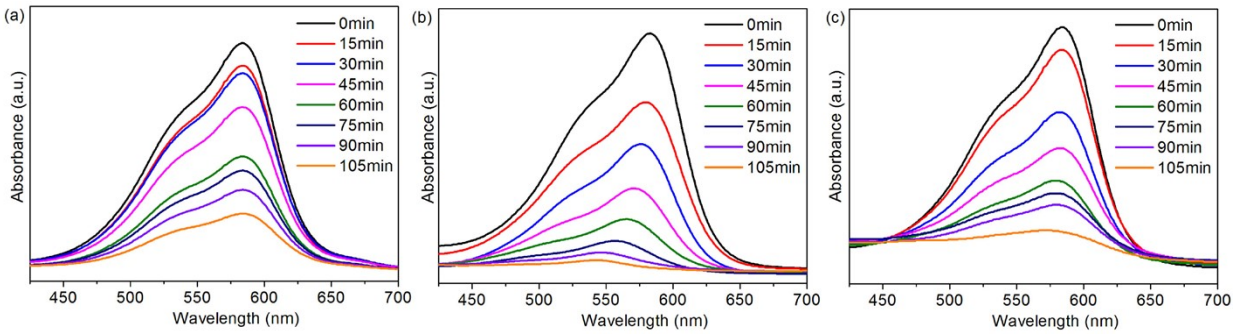

Fig. S9. Time dependent absorption spectra of **CV** solutions with photodegradation over compounds **1** (a), **2** (b) and **3** (c).

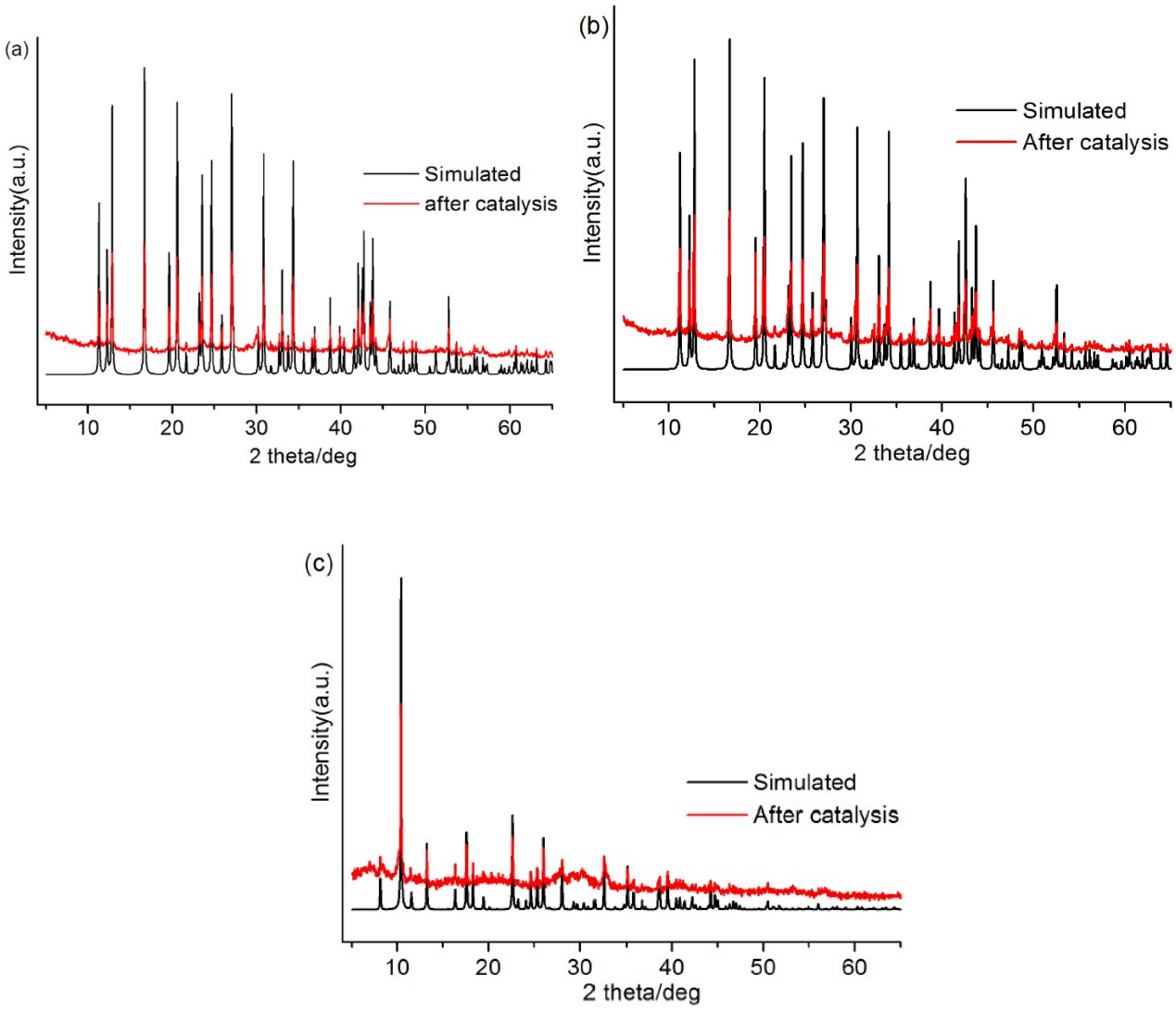

Fig. S10. Simulated PXRD patterns and experimental PXRD patterns after photocatalysis for compounds **1** (a), **2** (b) and **3** (c)

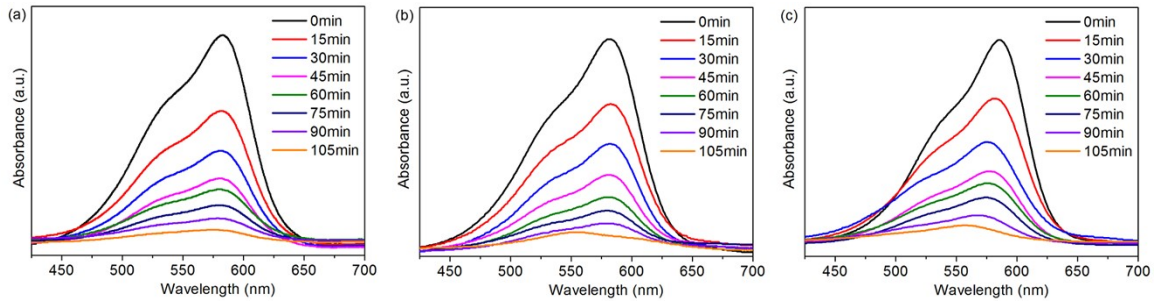

Fig. S11 Time dependent absorption spectra of **CV** solutions with photodegradation catalyzed by compound **2** in cycle 1 (a), cycle 2 (b) and cycle 3 (c).

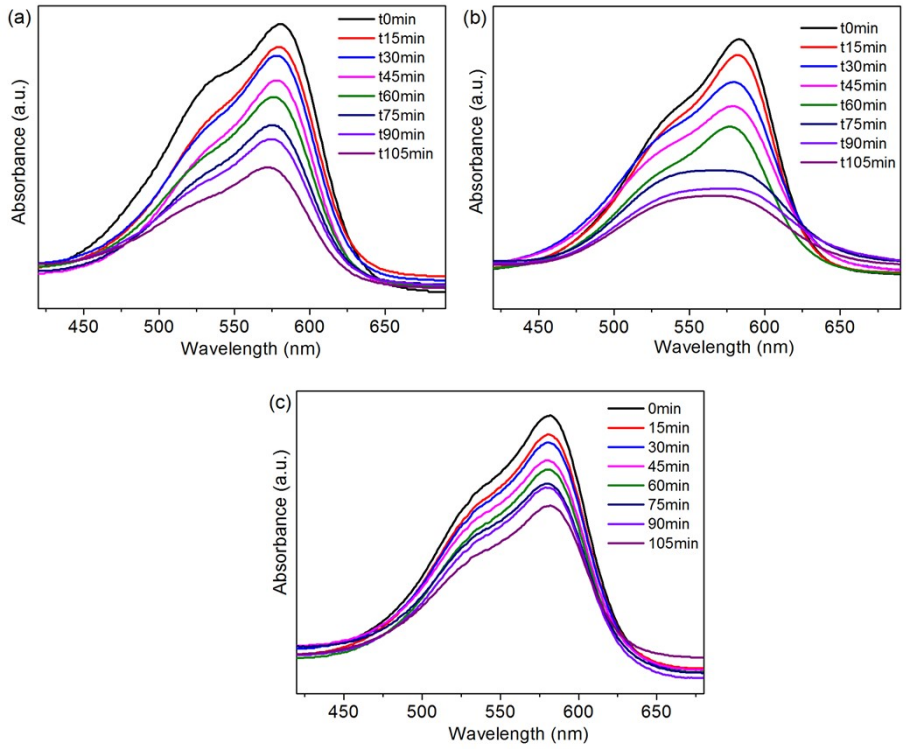

Fig. S12 Time dependent absorption spectra of CV solution with photodegradation catalyzed by compound **1** in the presence of radical quenching agents AO (a), BQ (b), and TBA (c).

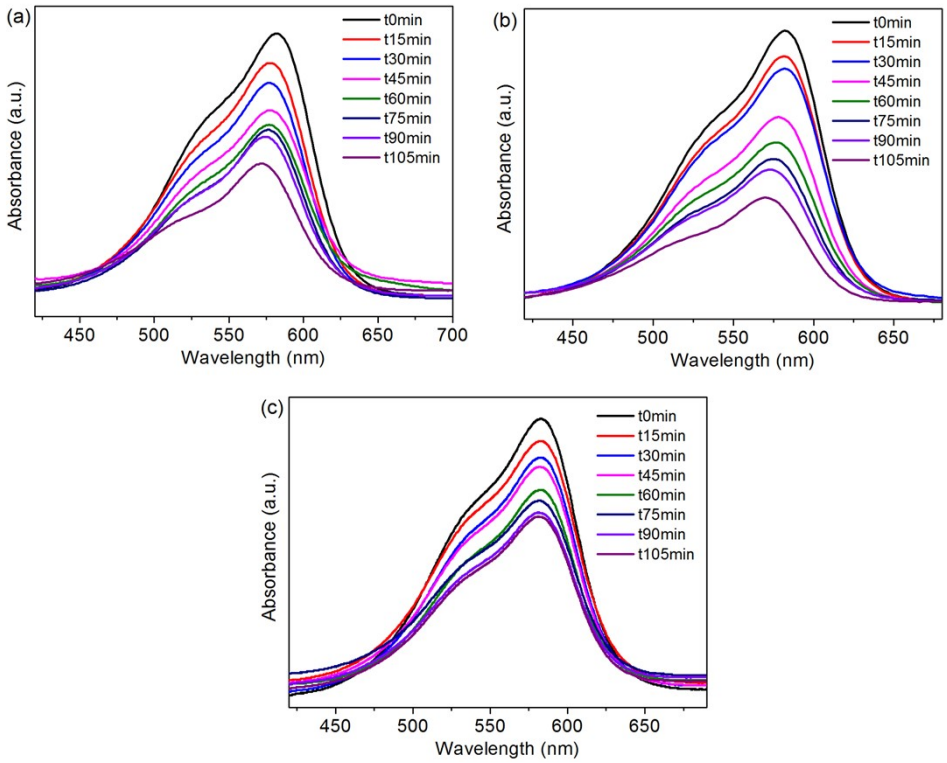

Fig. S13 Time dependent absorption spectra of CV solution with photodegradation catalyzed by compound **2** in the presence of radical quenching agents AO (a), BQ (b), and TBA (c).

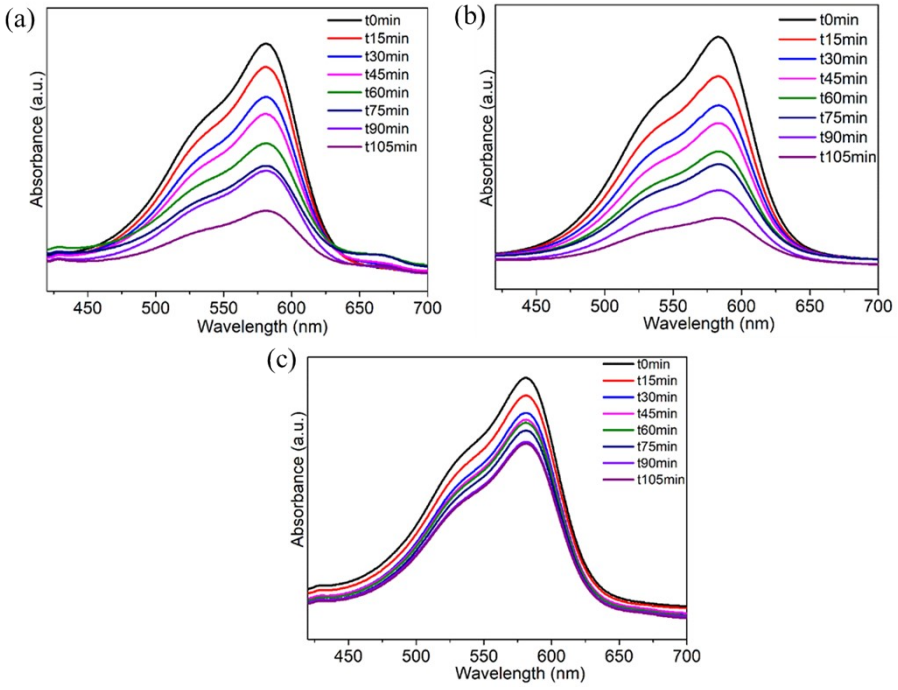

Fig. S14 Time dependent absorption spectra of CV solution with photodegradation catalyzed by compound **3** in the presence of radical quenching agents AO (a), BQ (b), and TBA (c).

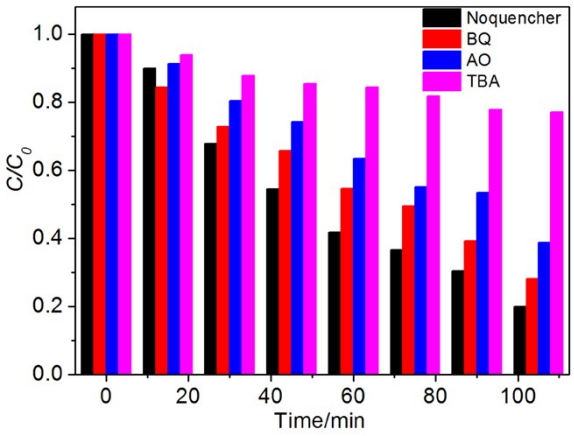

Fig. S15 Catalytic activities for photodegradation of CV over compound **3** in the presence of quenchers BQ, TBA and AO.

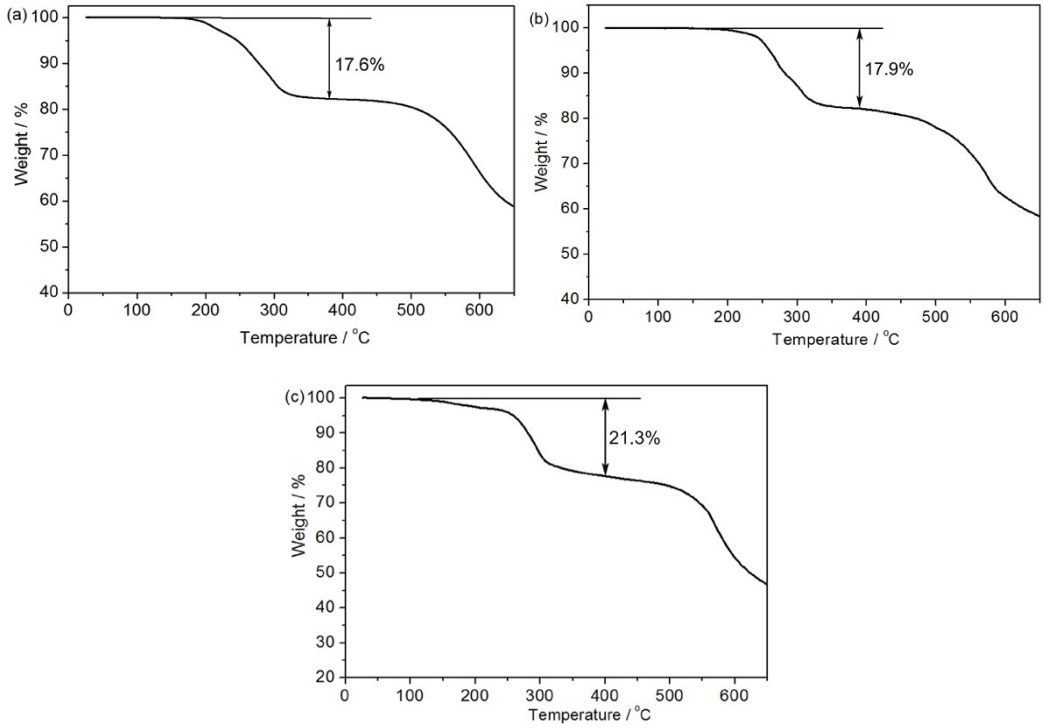

Fig. S16 Thermal gravimetric curves of compounds **1** (a), **2** (b), and **3** (c).

Thermal stabilities of compounds **1**–**3** were investigated using thermogravimetric analysis (TGA) method under a nitrogen atmosphere (Fig. S16). TGA curve shows that compound **1** has a mass loss of 17.6% between 190 and 400 °C, which is consistent with the theoretical mass loss of three en molecules (theoretical value: 18.7%). Compound **2** exhibits a similar decompostion process with a mass loss of 17.9 % between 180 °C and 400 °C (theoretical value: 18.8 % for 3 en). The total mass loss of 21.3 % in 110-400 °C of compound **3** is attributed to the loss of a H_2O and two dien molecules (theoretical value: 22.3%).